

Observation of $D \rightarrow \bar{K}_1(1270)\mu^+\nu_\mu$ and test of lepton flavor universality with $D \rightarrow \bar{K}_1(1270)\ell^+\nu_\ell$

M. Ablikim¹, M. N. Achasov^{4,c}, P. Adlarson⁷⁶, O. Afedulidis³, X. C. Ai⁸¹, R. Aliberti³⁵, A. Amoroso^{75A,75C}, Q. An^{72,58,a}, Y. Bai⁵⁷, O. Bakina³⁶, I. Balossino^{29A}, Y. Ban^{46,h}, H.-R. Bao⁶⁴, V. Batozskaya^{1,44}, K. Begzsuren³², N. Berger³⁵, M. Berlowski⁴⁴, M. Bertani^{28A}, D. Bettoni^{29A}, F. Bianchi^{75A,75C}, E. Bianco^{75A,75C}, A. Bortone^{75A,75C}, I. Boyko³⁶, R. A. Briere⁵, A. Brueggemann⁶⁹, H. Cai⁷⁷, X. Cai^{1,58}, A. Calcaterra^{28A}, G. F. Cao^{1,64}, N. Cao^{1,64}, S. A. Cetin^{62A}, X. Y. Chai^{46,h}, J. F. Chang^{1,58}, G. R. Che⁴³, Y. Z. Che^{1,58,64}, G. Chelkov^{36,b}, C. Chen⁴³, C. H. Chen⁹, Chao Chen⁵⁵, G. Chen¹, H. S. Chen^{1,64}, H. Y. Chen²⁰, M. L. Chen^{1,58,64}, S. J. Chen⁴², S. L. Chen⁴⁵, S. M. Chen⁶¹, T. Chen^{1,64}, X. R. Chen^{31,64}, X. T. Chen^{1,64}, Y. B. Chen^{1,58}, Y. Q. Chen³⁴, Z. J. Chen^{25,i}, Z. Y. Chen^{1,64}, S. K. Choi¹⁰, G. Cibinetto^{29A}, F. Cossio^{75C}, J. J. Cui⁵⁰, H. L. Dai^{1,58}, J. P. Dai⁷⁹, A. Dbeysi¹⁸, R. E. de Boer³, D. Dedovich³⁶, C. Q. Deng⁷³, Z. Y. Deng¹, A. Denig³⁵, I. Denysenko³⁶, M. Destefanis^{75A,75C}, F. De Mori^{75A,75C}, B. Ding^{67,1}, X. X. Ding^{46,h}, Y. Ding⁴⁰, Y. Ding³⁴, J. Dong^{1,58}, L. Y. Dong^{1,64}, M. Y. Dong^{1,58,64}, X. Dong⁷⁷, M. C. Du¹, S. X. Du⁸¹, Y. Y. Duan⁵⁵, Z. H. Duan⁴², P. Egorov^{36,b}, Y. H. Fan⁴⁵, J. Fang^{1,58}, J. Fang⁵⁹, S. S. Fang^{1,64}, W. X. Fang¹, Y. Fang¹, Y. Q. Fang^{1,58}, R. Farinelli^{29A}, L. Fava^{75B,75C}, F. Feldbauer³, G. Felici^{28A}, C. Q. Feng^{72,58}, J. H. Feng⁵⁹, Y. T. Feng^{72,58}, M. Fritsch³, C. D. Fu¹, J. L. Fu⁶⁴, Y. W. Fu^{1,64}, H. Gao⁶⁴, X. B. Gao⁴¹, Y. N. Gao^{46,h}, Yang Gao^{72,58}, S. Garbolino^{75C}, I. Garzia^{29A,29B}, L. Ge⁸¹, P. T. Ge¹⁹, Z. W. Ge⁴², C. Geng⁵⁹, E. M. Gersabeck⁶⁸, A. Gilman⁷⁰, K. Goetzen¹³, L. Gong⁴⁰, W. X. Gong^{1,58}, W. Gradi³⁵, S. Gramigna^{29A,29B}, M. Greco^{75A,75C}, M. H. Gu^{1,58}, Y. T. Gu¹⁵, C. Y. Guan^{1,64}, A. Q. Guo^{31,64}, L. B. Guo⁴¹, M. J. Guo⁵⁰, R. P. Guo⁴⁹, Y. P. Guo^{12,g}, A. Guskov^{36,b}, J. Gutierrez²⁷, K. L. Han⁶⁴, T. T. Han¹, F. Hanisch³, X. Q. Hao¹⁹, F. A. Harris⁶⁶, K. K. He⁵⁵, K. L. He^{1,64}, F. H. Heinlius³, C. H. Heinz³⁵, Y. K. Heng^{1,58,64}, C. Herold⁶⁰, T. Holtmann³, P. C. Hong³⁴, G. Y. Hou^{1,64}, X. T. Hou^{1,64}, Y. R. Hou⁶⁴, Z. L. Hou¹, B. Y. Hu⁵⁹, H. M. Hu^{1,64}, J. F. Hu^{56,j}, S. L. Hu^{12,g}, T. Hu^{1,58,64}, Y. Hu¹, G. S. Huang^{72,58}, K. X. Huang⁵⁹, L. Q. Huang^{31,64}, X. T. Huang⁵⁰, Y. P. Huang¹, Y. S. Huang⁵⁹, T. Hussain⁷⁴, F. Hölzken³, N. Hüskens³⁵, N. in der Wiesche⁶⁹, J. Jackson²⁷, S. Janchiv³², J. H. Jeong¹⁰, Q. Ji¹, Q. P. Ji¹⁹, W. Ji^{1,64}, X. B. Ji^{1,64}, X. L. Ji^{1,58}, Y. Y. Ji⁵⁰, X. Q. Jia⁵⁰, Z. K. Jia^{72,58}, D. Jiang^{1,64}, H. B. Jiang⁷⁷, P. C. Jiang^{46,h}, S. S. Jiang³⁹, T. J. Jiang¹⁶, X. S. Jiang^{1,58,64}, Y. Jiang⁶⁴, J. B. Jiao⁵⁰, J. K. Jiao³⁴, Z. Jiao²³, S. Jin⁴², Y. Jin⁶⁷, M. Q. Jing^{1,64}, X. M. Jing⁶⁴, T. Johansson⁷⁶, S. Kabana³³, N. Kalantar-Nayestanaki⁶⁵, X. L. Kang⁹, X. S. Kang⁴⁰, M. Kavatsyuk⁶⁵, B. C. Ke⁸¹, V. Khachatryan²⁷, A. Khoukaz⁶⁹, R. Kiuchi¹, O. B. Kolcu^{62A}, B. Kopf³, M. Kuessner³, X. Kui^{1,64}, N. Kumar²⁶, A. Kupsc^{44,76}, W. Kühn³⁷, J. J. Lane⁶⁸, L. Lavezzi^{75A,75C}, T. T. Lei^{72,58}, Z. H. Lei^{72,58}, M. Lellmann³⁵, T. Lenz³⁵, C. Li⁴³, C. Li⁴⁷, C. H. Li³⁹, Cheng Li^{72,58}, D. M. Li⁸¹, F. Li^{1,58}, G. Li¹, H. B. Li^{1,64}, H. J. Li¹⁹, H. N. Li^{56,j}, Hui Li⁴³, J. R. Li⁶¹, J. S. Li⁵⁹, K. Li¹, K. L. Li¹⁹, L. J. Li^{1,64}, L. K. Li¹, Lei Li⁴⁸, M. H. Li⁴³, P. R. Li^{38,k,l}, Q. M. Li^{1,64}, Q. X. Li⁵⁰, R. Li^{17,31}, S. X. Li¹², T. Li⁵⁰, W. D. Li^{1,64}, W. G. Li^{1,a}, X. Li^{1,64}, X. H. Li^{72,58}, X. L. Li⁵⁰, X. Y. Li^{1,64}, X. Z. Li⁵⁹, Y. G. Li^{46,h}, Z. J. Li⁵⁹, Z. Y. Li⁷⁹, C. Liang⁴², H. Liang^{1,64}, H. Liang^{72,58}, Y. F. Liang⁵⁴, Y. T. Liang^{31,64}, G. R. Liao¹⁴, Y. P. Liao^{1,64}, J. Libby²⁶, A. Limphirat⁶⁰, C. C. Lin⁵⁵, D. X. Lin^{31,64}, T. Lin¹, B. J. Liu¹, B. X. Liu⁷⁷, C. Liu³⁴, C. X. Liu¹, F. Liu¹, F. H. Liu⁶, G. M. Liu^{56,j}, H. Liu^{38,k,l}, H. B. Liu¹⁵, H. H. Liu¹, H. M. Liu^{1,64}, Huihui Liu²¹, J. B. Liu^{72,58}, J. Y. Liu^{1,64}, K. Liu^{38,k,l}, K. Y. Liu⁴⁰, Ke Liu²², L. Liu^{72,58}, L. C. Liu⁴³, Lu Liu⁴³, M. H. Liu^{12,g}, P. L. Liu¹, Q. Liu⁶⁴, S. B. Liu^{72,58}, T. Liu^{12,g}, W. K. Liu⁴³, W. M. Liu^{72,58}, X. Liu^{38,k,l}, X. Liu³⁹, Y. Liu⁸¹, Y. Liu^{38,k,l}, Y. B. Liu⁴³, Z. A. Liu^{1,58,64}, Z. D. Liu⁹, Z. Q. Liu⁵⁰, X. C. Lou^{1,58,64}, F. X. Lu⁵⁹, H. J. Lu²³, J. G. Lu^{1,58}, X. L. Lu¹, Y. Lu⁷, Y. P. Lu^{1,58}, Z. H. Lu^{1,64}, C. L. Luo⁴¹, J. R. Luo⁵⁹, M. X. Luo⁸⁰, T. Luo^{12,g}, X. L. Luo^{1,58}, X. R. Lyu⁶⁴, Y. F. Lyu⁴³, F. C. Ma⁴⁰, H. Ma⁷⁹, H. L. Ma¹, J. L. Ma^{1,64}, L. L. Ma⁵⁰, L. R. Ma⁶⁷, M. M. Ma^{1,64}, Q. M. Ma¹, R. Q. Ma^{1,64}, T. Ma^{72,58}, X. T. Ma^{1,64}, X. Y. Ma^{1,58}, Y. M. Ma³¹, F. E. Maas¹⁸, I. MacKay⁷⁰, M. Maggiora^{75A,75C}, S. Malde⁷⁰, Y. J. Mao^{46,h}, Z. P. Mao¹, S. Marcello^{75A,75C}, Z. X. Meng⁶⁷, J. G. Messchendorp^{13,65}, G. Mezzadri^{29A}, H. Miao^{1,64}, T. J. Min⁴², R. E. Mitchell²⁷, X. H. Mo^{1,58,64}, B. Moses²⁷, N. Yu. Muchnoi^{4,c}, J. Muskalla³⁵, Y. Nefedov³⁶, F. Nerling^{18,e}, L. S. Nie²⁰, I. B. Nikolaev^{4,c}, Z. Ning^{1,58}, S. Nisar^{11,m}, Q. L. Niu^{38,k,l}, W. D. Niu⁵⁵, Y. Niu⁵⁰, S. L. Olsen⁶⁴, S. L. Olsen^{10,64}, Q. Ouyang^{1,58,64}, S. Pacetti^{28B,28C}, X. Pan⁵⁵, Y. Pan⁵⁷, A. Pathak³⁴, Y. P. Pei^{72,58}, M. Pelizaeus³, H. P. Peng^{72,58}, Y. Y. Peng^{38,k,l}, K. Peters^{13,e}, J. L. Ping⁴¹, R. G. Ping^{1,64}, S. Plura³⁵, V. Prasad³³, F. Z. Qi¹, H. Qi^{72,58}, H. R. Qi⁶¹, M. Qi⁴², T. Y. Qi^{12,g}, S. Qian^{1,58}, W. B. Qian⁶⁴, C. F. Qiao⁶⁴, X. K. Qiao⁸¹, J. J. Qin⁷³, L. Q. Qin¹⁴, L. Y. Qin^{72,58}, X. P. Qin^{12,g}, X. S. Qin⁵⁰, Z. H. Qin^{1,58}, J. F. Qiu¹, Z. H. Qu⁷³, C. F. Redmer³⁵, K. J. Ren³⁹, A. Rivetti^{75C}, M. Roloff^{75C}, G. Rong^{1,64}, Ch. Rosner¹⁸, M. Q. Ruan^{1,58}, S. N. Ruan⁴³, N. Salone⁴⁴, A. Sarantsev^{36,d}, Y. Schelhaas³⁵, K. Schoenning⁷⁶, M. Scodeggio^{29A}, K. Y. Shan^{12,g}, W. Shan²⁴, X. Y. Shan^{72,58}, Z. J. Shang^{38,k,l}, J. F. Shangguan¹⁶, L. G. Shao^{1,64}, M. Shao^{72,58}, C. P. Shen^{12,g}, H. F. Shen^{1,8}, W. H. Shen⁶⁴,

X. Y. Shen^{1,64}, B. A. Shi⁶⁴, H. Shi^{72,58}, H. C. Shi^{72,58}, J. L. Shi^{12,g}, J. Y. Shi¹, Q. Q. Shi⁵⁵, S. Y. Shi⁷³, X. Shi^{1,58}, J. J. Song¹⁹, T. Z. Song⁵⁹, W. M. Song^{34,1}, Y. J. Song^{12,g}, Y. X. Song^{46,h,n}, S. Sosio^{75A,75C}, S. Spataro^{75A,75C}, F. Stieler³⁵, S. S. Su⁴⁰, Y. J. Su⁶⁴, G. B. Sun⁷⁷, G. X. Sun¹, H. Sun⁶⁴, H. K. Sun¹, J. F. Sun¹⁹, K. Sun⁶¹, L. Sun⁷⁷, S. S. Sun^{1,64}, T. Sun^{51,f}, W. Y. Sun³⁴, Y. Sun⁹, Y. J. Sun^{72,58}, Y. Z. Sun¹, Z. Q. Sun^{1,64}, Z. T. Sun⁵⁰, C. J. Tang⁵⁴, G. Y. Tang¹, J. Tang⁵⁹, M. Tang^{72,58}, Y. A. Tang⁷⁷, L. Y. Tao⁷³, Q. T. Tao^{25,i}, M. Tat⁷⁰, J. X. Teng^{72,58}, V. Thoren⁷⁶, W. H. Tian⁵⁹, Y. Tian^{31,64}, Z. F. Tian⁷⁷, I. Uman^{62B}, Y. Wan⁵⁵, S. J. Wang⁵⁰, B. Wang¹, B. L. Wang⁶⁴, Bo Wang^{72,58}, D. Y. Wang^{46,h}, F. Wang⁷³, H. J. Wang^{38,k,l}, J. J. Wang⁷⁷, J. P. Wang⁵⁰, K. Wang^{1,58}, L. L. Wang¹, M. Wang⁵⁰, N. Y. Wang⁶⁴, S. Wang^{38,k,l}, S. Wang^{12,g}, T. Wang^{12,g}, T. J. Wang⁴³, W. Wang⁷³, W. Wang⁵⁹, W. P. Wang^{35,58,72,o}, X. Wang^{46,h}, X. F. Wang^{38,k,l}, X. J. Wang³⁹, X. L. Wang^{12,g}, X. N. Wang¹, Y. Wang⁶¹, Y. D. Wang⁴⁵, Y. F. Wang^{1,58,64}, Y. L. Wang¹⁹, Y. N. Wang⁴⁵, Y. Q. Wang¹, Yaqian Wang¹⁷, Yi Wang⁶¹, Z. Wang^{1,58}, Z. L. Wang⁷³, Z. Y. Wang^{1,64}, Ziyi Wang⁶⁴, D. H. Wei¹⁴, F. Weidner⁶⁹, S. P. Wen¹, Y. R. Wen³⁹, U. Wiedner³, G. Wilkinson⁷⁰, M. Wolke⁷⁶, L. Wollenberg³, C. Wu³⁹, J. F. Wu^{1,8}, L. H. Wu¹, L. J. Wu^{1,64}, X. Wu^{12,g}, X. H. Wu³⁴, Y. Wu^{72,58}, Y. H. Wu⁵⁵, Y. J. Wu³¹, Z. Wu^{1,58}, L. Xia^{72,58}, X. M. Xian³⁹, B. H. Xiang^{1,64}, T. Xiang^{46,h}, D. Xiao^{38,k,l}, G. Y. Xiao⁴², S. Y. Xiao¹, Y. L. Xiao^{12,g}, Z. J. Xiao⁴¹, C. Xie⁴², X. H. Xie^{46,h}, Y. Xie⁵⁰, Y. G. Xie^{1,58}, Y. H. Xie⁶, Z. P. Xie^{72,58}, T. Y. Xing^{1,64}, C. F. Xu^{1,64}, C. J. Xu⁵⁹, G. F. Xu¹, H. Y. Xu^{67,2,p}, M. Xu^{72,58}, Q. J. Xu¹⁶, Q. N. Xu³⁰, W. Xu¹, W. L. Xu⁶⁷, X. P. Xu⁵⁵, Y. Xu⁴⁰, Y. C. Xu⁷⁸, Z. S. Xu⁶⁴, F. Yan^{12,g}, L. Yan^{12,g}, W. B. Yan^{72,58}, W. C. Yan⁸¹, X. Q. Yan^{1,64}, H. J. Yang^{51,f}, H. L. Yang³⁴, H. X. Yang¹, T. Yang¹, Y. Yang^{12,g}, Y. F. Yang^{1,64}, Y. F. Yang⁴³, Y. X. Yang^{1,64}, Z. W. Yang^{38,k,l}, Z. P. Yao⁵⁰, M. Ye^{1,58}, M. H. Ye⁸, J. H. Yin¹, Junhao Yin⁴³, Z. Y. You⁵⁹, B. X. Yu^{1,58,64}, C. X. Yu⁴³, G. Yu^{1,64}, J. S. Yu^{25,i}, M. C. Yu⁴⁰, T. Yu⁷³, X. D. Yu^{46,h}, Y. C. Yu⁸¹, C. Z. Yuan^{1,64}, J. Yuan³⁴, J. Yuan⁴⁵, L. Yuan², S. C. Yuan^{1,64}, Y. Yuan^{1,64}, Z. Y. Yuan⁵⁹, C. X. Yue³⁹, A. A. Zafar⁷⁴, F. R. Zeng⁵⁰, S. H. Zeng^{63A,63B,63C,63D}, X. Zeng^{12,g}, Y. Zeng^{25,i}, Y. J. Zeng^{1,64}, X. Y. Zhai³⁴, Y. C. Zhai⁵⁰, Y. H. Zhan⁵⁹, A. Q. Zhang^{1,64}, B. L. Zhang^{1,64}, B. X. Zhang¹, D. H. Zhang⁴³, G. Y. Zhang¹⁹, H. Zhang⁸¹, H. Zhang^{72,58}, H. C. Zhang^{1,58,64}, H. H. Zhang³⁴, H. H. Zhang⁵⁹, H. Q. Zhang^{1,58,64}, H. R. Zhang^{72,58}, H. Y. Zhang^{1,58}, J. Zhang⁵⁹, J. Zhang⁸¹, J. J. Zhang⁵², J. L. Zhang²⁰, J. Q. Zhang⁴¹, J. S. Zhang^{12,g}, J. W. Zhang^{1,58,64}, J. X. Zhang^{38,k,l}, J. Y. Zhang¹, J. Z. Zhang^{1,64}, Jianyu Zhang⁶⁴, L. M. Zhang⁶¹, Lei Zhang⁴², P. Zhang^{1,64}, Q. Y. Zhang³⁴, R. Y. Zhang^{38,k,l}, S. H. Zhang^{1,64}, Shulei Zhang^{25,i}, X. M. Zhang¹, X. Y. Zhang⁴⁰, X. Y. Zhang⁵⁰, Y. Zhang¹, Y. Zhang⁷³, Y. T. Zhang⁸¹, Y. H. Zhang^{1,58}, Y. M. Zhang³⁹, Yan Zhang^{72,58}, Z. D. Zhang¹, Z. H. Zhang¹, Z. L. Zhang³⁴, Z. Y. Zhang⁷⁷, Z. Y. Zhang⁴³, Z. Z. Zhang⁴⁵, G. Zhao¹, J. Y. Zhao^{1,64}, J. Z. Zhao^{1,58}, L. Zhao¹, Lei Zhao^{72,58}, M. G. Zhao⁴³, N. Zhao⁷⁹, R. P. Zhao⁶⁴, S. J. Zhao⁸¹, Y. B. Zhao^{1,58}, Y. X. Zhao^{31,64}, Z. G. Zhao^{72,58}, A. Zhemchugov^{36,b}, B. Zheng⁷³, B. M. Zheng³⁴, J. P. Zheng^{1,58}, W. J. Zheng^{1,64}, Y. H. Zheng⁶⁴, B. Zhong⁴¹, X. Zhong⁵⁹, H. Zhou⁵⁰, J. Y. Zhou³⁴, L. P. Zhou^{1,64}, S. Zhou⁶, X. Zhou⁷⁷, X. K. Zhou⁶, X. R. Zhou^{72,58}, X. Y. Zhou³⁹, Y. Z. Zhou^{12,g}, Z. C. Zhou²⁰, A. N. Zhu⁶⁴, J. Zhu⁴³, K. Zhu¹, K. J. Zhu^{1,58,64}, K. S. Zhu^{12,g}, L. Zhu³⁴, L. X. Zhu⁶⁴, S. H. Zhu⁷¹, T. J. Zhu^{12,g}, W. D. Zhu⁴¹, Y. C. Zhu^{72,58}, Z. A. Zhu^{1,64}, J. H. Zou¹, J. Zu^{72,58}

(BESIII Collaboration)

¹ Institute of High Energy Physics, Beijing 100049, People's Republic of China

² Beihang University, Beijing 100191, People's Republic of China

³ Bochum Ruhr-University, D-44780 Bochum, Germany

⁴ Budker Institute of Nuclear Physics SB RAS (BINP), Novosibirsk 630090, Russia

⁵ Carnegie Mellon University, Pittsburgh, Pennsylvania 15213, USA

⁶ Central China Normal University, Wuhan 430079, People's Republic of China

⁷ Central South University, Changsha 410083, People's Republic of China

⁸ China Center of Advanced Science and Technology, Beijing 100190, People's Republic of China

⁹ China University of Geosciences, Wuhan 430074, People's Republic of China

¹⁰ Chung-Ang University, Seoul, 06974, Republic of Korea

¹¹ COMSATS University Islamabad, Lahore Campus, Defence Road, Off Raiwind Road, 54000 Lahore, Pakistan

¹² Fudan University, Shanghai 200433, People's Republic of China

¹³ GSI Helmholtzcentre for Heavy Ion Research GmbH, D-64291 Darmstadt, Germany

¹⁴ Guangxi Normal University, Guilin 541004, People's Republic of China

¹⁵ Guangxi University, Nanning 530004, People's Republic of China

¹⁶ Hangzhou Normal University, Hangzhou 310036, People's Republic of China

¹⁷ Hebei University, Baoding 071002, People's Republic of China

¹⁸ Helmholtz Institute Mainz, Staudinger Weg 18, D-55099 Mainz, Germany

- ¹⁹ Henan Normal University, Xinxiang 453007, People's Republic of China
²⁰ Henan University, Kaifeng 475004, People's Republic of China
²¹ Henan University of Science and Technology, Luoyang 471003, People's Republic of China
²² Henan University of Technology, Zhengzhou 450001, People's Republic of China
²³ Huangshan College, Huangshan 245000, People's Republic of China
²⁴ Hunan Normal University, Changsha 410081, People's Republic of China
²⁵ Hunan University, Changsha 410082, People's Republic of China
²⁶ Indian Institute of Technology Madras, Chennai 600036, India
²⁷ Indiana University, Bloomington, Indiana 47405, USA
²⁸ INFN Laboratori Nazionali di Frascati , (A)INFN Laboratori Nazionali di Frascati, I-00044, Frascati, Italy; (B)INFN Sezione di Perugia, I-06100, Perugia, Italy; (C)University of Perugia, I-06100, Perugia, Italy
²⁹ INFN Sezione di Ferrara, (A)INFN Sezione di Ferrara, I-44122, Ferrara, Italy; (B)University of Ferrara, I-44122, Ferrara, Italy
³⁰ Inner Mongolia University, Hohhot 010021, People's Republic of China
³¹ Institute of Modern Physics, Lanzhou 730000, People's Republic of China
³² Institute of Physics and Technology, Peace Avenue 54B, Ulaanbaatar 13330, Mongolia
³³ Instituto de Alta Investigación, Universidad de Tarapacá, Casilla 7D, Arica 1000000, Chile
³⁴ Jilin University, Changchun 130012, People's Republic of China
³⁵ Johannes Gutenberg University of Mainz, Johann-Joachim-Becher-Weg 45, D-55099 Mainz, Germany
³⁶ Joint Institute for Nuclear Research, 141980 Dubna, Moscow region, Russia
³⁷ Justus-Liebig-Universitaet Giessen, II. Physikalisches Institut, Heinrich-Buff-Ring 16, D-35392 Giessen, Germany
³⁸ Lanzhou University, Lanzhou 730000, People's Republic of China
³⁹ Liaoning Normal University, Dalian 116029, People's Republic of China
⁴⁰ Liaoning University, Shenyang 110036, People's Republic of China
⁴¹ Nanjing Normal University, Nanjing 210023, People's Republic of China
⁴² Nanjing University, Nanjing 210093, People's Republic of China
⁴³ Nankai University, Tianjin 300071, People's Republic of China
⁴⁴ National Centre for Nuclear Research, Warsaw 02-093, Poland
⁴⁵ North China Electric Power University, Beijing 102206, People's Republic of China
⁴⁶ Peking University, Beijing 100871, People's Republic of China
⁴⁷ Qufu Normal University, Qufu 273165, People's Republic of China
⁴⁸ Renmin University of China, Beijing 100872, People's Republic of China
⁴⁹ Shandong Normal University, Jinan 250014, People's Republic of China
⁵⁰ Shandong University, Jinan 250100, People's Republic of China
⁵¹ Shanghai Jiao Tong University, Shanghai 200240, People's Republic of China
⁵² Shanxi Normal University, Linfen 041004, People's Republic of China
⁵³ Shanxi University, Taiyuan 030006, People's Republic of China
⁵⁴ Sichuan University, Chengdu 610064, People's Republic of China
⁵⁵ Soochow University, Suzhou 215006, People's Republic of China
⁵⁶ South China Normal University, Guangzhou 510006, People's Republic of China
⁵⁷ Southeast University, Nanjing 211100, People's Republic of China
⁵⁸ State Key Laboratory of Particle Detection and Electronics, Beijing 100049, Hefei 230026, People's Republic of China
⁵⁹ Sun Yat-Sen University, Guangzhou 510275, People's Republic of China
⁶⁰ Suranaree University of Technology, University Avenue 111, Nakhon Ratchasima 30000, Thailand
⁶¹ Tsinghua University, Beijing 100084, People's Republic of China
⁶² Turkish Accelerator Center Particle Factory Group, (A)Istinye University, 34010, Istanbul, Turkey; (B)Near East University, Nicosia, North Cyprus, 99138, Mersin 10, Turkey
⁶³ University of Bristol, H H Wills Physics Laboratory, Tyndall Avenue, Bristol, BS8 1TL, UK
⁶⁴ University of Chinese Academy of Sciences, Beijing 100049, People's Republic of China
⁶⁵ University of Groningen, NL-9747 AA Groningen, The Netherlands
⁶⁶ University of Hawaii, Honolulu, Hawaii 96822, USA
⁶⁷ University of Jinan, Jinan 250022, People's Republic of China

⁶⁸ University of Manchester, Oxford Road, Manchester, M13 9PL, United Kingdom

⁶⁹ University of Muenster, Wilhelm-Klemm-Strasse 9, 48149 Muenster, Germany

⁷⁰ University of Oxford, Keble Road, Oxford OX13RH, United Kingdom

⁷¹ University of Science and Technology Liaoning, Anshan 114051, People's Republic of China

⁷² University of Science and Technology of China, Hefei 230026, People's Republic of China

⁷³ University of South China, Hengyang 421001, People's Republic of China

⁷⁴ University of the Punjab, Lahore-54590, Pakistan

⁷⁵ University of Turin and INFN, (A)University of Turin, I-10125, Turin, Italy; (B)University of Eastern Piedmont, I-15121, Alessandria, Italy; (C)INFN, I-10125, Turin, Italy

⁷⁶ Uppsala University, Box 516, SE-75120 Uppsala, Sweden

⁷⁷ Wuhan University, Wuhan 430072, People's Republic of China

⁷⁸ Yantai University, Yantai 264005, People's Republic of China

⁷⁹ Yunnan University, Kunming 650500, People's Republic of China

⁸⁰ Zhejiang University, Hangzhou 310027, People's Republic of China

⁸¹ Zhengzhou University, Zhengzhou 450001, People's Republic of China

^a Deceased

^b Also at the Moscow Institute of Physics and Technology, Moscow 141700, Russia

^c Also at the Novosibirsk State University, Novosibirsk, 630090, Russia

^d Also at the NRC "Kurchatov Institute", PNPI, 188300, Gatchina, Russia

^e Also at Goethe University Frankfurt, 60323 Frankfurt am Main, Germany

^f Also at Key Laboratory for Particle Physics, Astrophysics and Cosmology, Ministry of Education; Shanghai Key Laboratory for Particle Physics and Cosmology; Institute of Nuclear and Particle Physics, Shanghai 200240, People's Republic of China

^g Also at Key Laboratory of Nuclear Physics and Ion-beam Application (MOE) and Institute of Modern Physics, Fudan University, Shanghai 200443, People's Republic of China

^h Also at State Key Laboratory of Nuclear Physics and Technology, Peking University, Beijing 100871, People's Republic of China

ⁱ Also at School of Physics and Electronics, Hunan University, Changsha 410082, China

^j Also at Guangdong Provincial Key Laboratory of Nuclear Science, Institute of Quantum Matter, South China Normal University, Guangzhou 510006, China

^k Also at MOE Frontiers Science Center for Rare Isotopes, Lanzhou University, Lanzhou 730000, People's Republic of China

^l Also at Lanzhou Center for Theoretical Physics, Lanzhou University, Lanzhou 730000, People's Republic of China

^m Also at the Department of Mathematical Sciences, IBA, Karachi 75270, Pakistan

ⁿ Also at Ecole Polytechnique Federale de Lausanne (EPFL), CH-1015 Lausanne, Switzerland

^o Also at Helmholtz Institute Mainz, Staudinger Weg 18, D-55099 Mainz, Germany

^p Also at School of Physics, Beihang University, Beijing 100191, China

By analyzing 7.93 fb^{-1} of e^+e^- collision data collected at the center-of-mass energy of 3.773 GeV with the BESIII detector operated at the BEPCII collider, we report the observation of the semimuonic decays of $D^+ \rightarrow \bar{K}_1(1270)^0 \mu^+ \nu_\mu$ and $D^0 \rightarrow K_1(1270)^- \mu^+ \nu_\mu$ with statistical significances of 12.5σ and 6.0σ , respectively. Their decay branching fractions are determined to be $\mathcal{B}[D^+ \rightarrow \bar{K}_1(1270)^0 \mu^+ \nu_\mu] = (2.36 \pm 0.20^{+0.18}_{-0.27} \pm 0.48) \times 10^{-3}$ and $\mathcal{B}[D^0 \rightarrow K_1(1270)^- \mu^+ \nu_\mu] = (0.78 \pm 0.11^{+0.05}_{-0.09} \pm 0.15) \times 10^{-3}$, where the first and second uncertainties are statistical and systematic, respectively, and the third originates from the input branching fraction of $\bar{K}_1(1270)^0 \rightarrow K^-\pi^+\pi^0$ or $K_1(1270)^- \rightarrow K^-\pi^+\pi^-$. Combining our branching fractions with the previous measurements of $\mathcal{B}[D^+ \rightarrow \bar{K}_1(1270)^0 e^+ \nu_e]$ and $\mathcal{B}[D^0 \rightarrow K_1(1270)^- e^+ \nu_e]$, we determine the branching fraction ratios to be $\mathcal{B}[D^+ \rightarrow \bar{K}_1(1270)^0 \mu^+ \nu_\mu]/\mathcal{B}[D^+ \rightarrow \bar{K}_1(1270)^0 e^+ \nu_e] = 1.03 \pm 0.14^{+0.11}_{-0.15}$ and $\mathcal{B}[D^0 \rightarrow K_1(1270)^- \mu^+ \nu_\mu]/\mathcal{B}[D^0 \rightarrow K_1(1270)^- e^+ \nu_e] = 0.74 \pm 0.13^{+0.08}_{-0.13}$. Using the branching fractions measured in this work and the world-average lifetimes of the D^+ and D^0 mesons, we determine the semimuonic partial decay width ratio to be $\Gamma[D^+ \rightarrow \bar{K}_1(1270)^0 \mu^+ \nu_\mu]/\Gamma[D^0 \rightarrow K_1(1270)^- \mu^+ \nu_\mu] = 1.22 \pm 0.10^{+0.06}_{-0.09}$, which is consistent with unity as predicted by isospin conservation.

Experimental studies of the semileptonic (SL) decays of charmed mesons are important to deeply understand

nonperturbative strong-interaction dynamics in weak decays. The SL D transitions into $\bar{K}_1(1270)$ offer an

clean window to access the $K_1(1270)$ and $K_1(1400)$, which are mixtures of the 1^3P_1 and 1^1P_1 states of K_1 with mixing angle θ_{K_1} . The determination of θ_{K_1} is essential for the theoretical description of τ [1], B [2, 3], and D [4–6] decays into axial-vector strange mesons. Throughout this paper, charged-conjugate modes are implied and K_1 denotes $K_1(1270)$ unless stated otherwise.

Branching fractions (BFs) for $D^{+(0)} \rightarrow \bar{K}_1 \ell^+ \nu_\ell (\ell = e \text{ or } \mu)$ were calculated in the Isgur-Scora-Grinstein-Wise (ISGW) quark model [7] and its update with ISGW2 [8]. The BFs for $D^+ \rightarrow \bar{K}_1 \mu^+ \nu_\mu$ and $D^0 \rightarrow \bar{K}_1 \mu^+ \nu_\mu$ were predicted to be 0.1% and 0.3%, respectively. However, this model ignores mixing between 1P_1 and 3P_1 states. Recently, the BFs of $D^{+(0)} \rightarrow \bar{K}_1 \ell^+ \nu_\ell$ were calculated with other theoretical approaches, including three-point quantum chromodynamics (QCD) sum rules (3PSR) [9], the covariant light-front quark model (CLFQM) [10], and light-cone QCD sum rules (LCSR) [11]. In general, the predicted BFs range from 10^{-3} to 10^{-2} [9–12], and are sensitive to both the amplitude and sign of θ_{K_1} . Measurements of the BFs of $D^{+(0)} \rightarrow \bar{K}_1 \mu^+ \nu_\mu$ are important to test these theoretical calculations, to explore the nature of axial-vector strange mesons, and to understand the weak-decay mechanisms of D mesons.

Lepton flavor universality (LFU) is a basic feature of the standard model (SM), in which the couplings between the three families of leptons and the gauge bosons are independent of lepton family. Nevertheless, a few hints of tension between experimental measurements and SM predictions have been reported in some cases, including SL B decays [13] and the Cabibbo-angle anomaly [14, 15]. Intensive tests of LFU in different SL decays of heavy mesons are important to understand these anomalies. Reference [16] notes that there may indeed be observable LFU violation effects in the SL decays mediated via $c \rightarrow s\ell^+ \nu_\ell$. In the SM, the ratio $\mathcal{R}_{\mu/e}^{\bar{K}_1} = \mathcal{B}_{D \rightarrow \bar{K}_1 \mu^+ \nu_\mu} / \mathcal{B}_{D \rightarrow \bar{K}_1 e^+ \nu_e}$ is predicted to be 0.95–0.99 [9–12]. To date, no experimental study of the semimuonic $D^{+(0)}$ decays into axial-vector mesons has been reported, and LFU in the SL $D^{+(0)}$ decays into axial-vector mesons has never been tested [17]. Observation of the decays and measurements of the BFs of $D^+ \rightarrow \bar{K}_1^0 \mu^+ \nu_\mu$ and $D^0 \rightarrow \bar{K}_1^- \mu^+ \nu_\mu$ offer an important opportunity to test $\mu\text{-}e$ LFU.

This paper reports the first observation of $D^+ \rightarrow \bar{K}_1^0 \mu^+ \nu_\mu$ and $D^0 \rightarrow \bar{K}_1^- \mu^+ \nu_\mu$ by using an e^+e^- collision data sample corresponding to an integrated luminosity of 7.93 fb^{-1} [18], recorded at the center-of-mass energy of $\sqrt{s} = 3.773 \text{ GeV}$ with the BESIII detector [19]. Using our BFs and the world average BFs of $D^+ \rightarrow \bar{K}_1^0 e^+ \nu_e$, we provide the first test of the $\mu\text{-}e$ LFU with $D^+ \rightarrow \bar{K}_1^0 \ell^+ \nu_\ell$. Combining the BFs of $D^+ \rightarrow \bar{K}_1^0 \mu^+ \nu_\mu$ and $D^0 \rightarrow \bar{K}_1^- \mu^+ \nu_\mu$ with the lifetimes of the D^+ and D^0 , we test isospin invariance in $D \rightarrow \bar{K}_1 \mu^+ \nu_\mu$ decays.

A description of the design and performance of the BESIII detector can be found in Ref. [19]. The end cap TOF system was upgraded in 2015 using multigap resistive plate chamber technology, providing a time

resolution of 60 ps [20], which benefits 67% of the data used in this analysis.

Simulated data samples are produced with a GEANT4-based [21] Monte Carlo (MC) toolkit including the geometric description of the BESIII detector and the detector response. The simulation includes the beam energy spread and initial state radiation (ISR) in the e^+e^- annihilations with the generator KKMC [22]. In the MC simulation, the production of open-charm processes directly produced via e^+e^- annihilations are modeled with the generator CONEXC [23]. The ISR production of vector charmonium(like) states and the continuum processes are incorporated in KKMC [22]. All particle decays are modeled with EVTGEN [24] using BFs either taken from the Particle Data Group [25], when available, or otherwise estimated with LUNDCHARM [26]. Final state radiation from charged final state particles is incorporated using PHOTOS [27]. The signal MC events of $D^{+(0)} \rightarrow K^-\pi^+\pi^{0(-)}\mu^+\nu_\mu$ are generated with a special MC generator developed from the amplitude analysis of $D^{+(0)} \rightarrow K^-\pi^+\pi^{0(-)}e^+\nu_e$ [28].

This work analyzes the $e^+e^- \rightarrow \psi(3770) \rightarrow D\bar{D}$ decay chain. The single-tag (ST) candidate events are selected by reconstructing a D^- or \bar{D}^0 in the hadronic final states $D^- \rightarrow K^+\pi^-\pi^-$, $K_S^0\pi^-$, $K^+\pi^-\pi^-\pi^0$, $K_S^0\pi^-\pi^0$, $K_S^0\pi^+\pi^-\pi^-$, $K^+K^-\pi^-$, or $\bar{D}^0 \rightarrow K^+\pi^-$, $K^+\pi^-\pi^0$, $K^+\pi^-\pi^-\pi^+$. These inclusively selected candidates are referred to as ST D^- (\bar{D}^0) mesons. In the presence of the ST D^- (\bar{D}^0) mesons, candidates for the signal decays are selected to form double-tag (DT) events. The BF of the semimuonic decay is determined by

$$\mathcal{B}_{\text{SL}} = N_{\text{DT}} / (N_{\text{ST}}^{\text{tot}} \cdot \varepsilon_{\text{sig}} \cdot \mathcal{B}_{K_1}), \quad (1)$$

where $N_{\text{ST}}^{\text{tot}}$ and N_{DT} are the total ST and DT yields in the data sample, $\varepsilon_{\text{sig}} = \Sigma_i [(\varepsilon_{\text{DT}}^i N_{\text{ST}}^i) / (\varepsilon_{\text{ST}}^i N_{\text{ST}}^{\text{tot}})]$ is the efficiency of detecting the semimuonic decay in the presence of the ST D^- (\bar{D}^0) meson and \mathcal{B}_{K_1} is the BF of $\bar{K}_1 \rightarrow K^-\pi^+\pi^{0(-)}$. Here, i denotes the ST mode, and ε_{ST} and ε_{DT} are efficiencies for selecting the ST and DT candidates, respectively.

The selection criteria of K^\pm , π^\pm , K_S^0 , and π^0 are the same as those used in Ref. [29]. The ST \bar{D} (\bar{D} denotes D^- or \bar{D}^0) mesons are selected based on two kinematic variables in the e^+e^- center-of-mass frame: the energy difference $\Delta E \equiv E_{\bar{D}} - E_{\text{beam}}$ and the beam-constrained mass $M_{\text{BC}} \equiv \sqrt{E_{\text{beam}}^2/c^4 - |\vec{p}_{\bar{D}}|^2/c^2}$. Here, E_{beam} is the beam energy, and $E_{\bar{D}}$ and $\vec{p}_{\bar{D}}$ are the total energy and momentum of the \bar{D} candidate, respectively. If there are multiple combinations for a given ST mode, the one giving the minimum $|\Delta E|$ is retained.

For each tag mode, the yield of reconstructed \bar{D} mesons is obtained from an unbinned maximum likelihood fit to its M_{BC} distribution. In the fit, the signal distribution is modeled by the simulated shape convolved with a double-Gaussian resolution function to model the resolution difference between the data and the MC simulation. The combinatorial backgrounds are parametrized by

an ARGUS function [30] with the endpoint fixed at $E_{\text{beam}} = 1.8865 \text{ GeV}$.

The candidates with M_{BC} within $(1.863, 1.877) \text{ GeV}/c^2$ for ST D^- and $(1.859, 1.873) \text{ GeV}/c^2$ for ST \bar{D}^0 are kept for further analyses. For detailed information about the ΔE requirements, the ST yields in data, and the ST efficiencies, see Table 1 of the Supplemental Material [31]. Summing over all tag modes, we obtain the total yields of ST D^- and \bar{D}^0 mesons to be $(4149.9 \pm 2.3_{\text{stat}}) \times 10^3$ and $(6306.8 \pm 2.8_{\text{stat}}) \times 10^3$, respectively.

Candidates for $D^+ \rightarrow \bar{K}_1^0 \mu^+ \nu_\mu$ or $D^0 \rightarrow K_1^- \mu^+ \nu_\mu$ are reconstructed from the remaining tracks and showers not used in the D^- or \bar{D}^0 ST selection. The \bar{K}_1^0 or K_1^- meson is reconstructed using its dominant decay $\bar{K}_1^0 \rightarrow K^- \pi^+ \pi^0$ or $K_1^- \rightarrow K^- \pi^+ \pi^-$. Candidates for K^-, π^\pm and π^0 are selected with the same criteria as those used in the ST selection. To identify muon candidates, we use the information from dE/dx , the time-of-flight system (TOF), and the electromagnetic calorimeter (EMC), and combined confidence levels for the muon, pion, and kaon hypotheses (CL_μ , CL_π and CL_K) are calculated. Muon candidates are required to satisfy $CL_\mu > 0.001$, $CL_\mu > CL_K$ and $CL_\mu > CL_\pi$. To reduce the background from hadrons, muon candidates are also required to have a deposited energy in the EMC within less than 0.28 GeV . The DT candidates must not contain any additional charged tracks, $N_{\text{char}}^{\text{extra}} = 0$; otherwise they are vetoed.

To suppress the backgrounds containing extra π^0 mesons, such as the hadronic decays $D^+ \rightarrow K^- \pi^+ \pi^+ \pi^0 \pi^0$ and $D^0 \rightarrow K^- \pi^+ \pi^- \pi^+ \pi^0$, we require that there are no additional combinations of two photons that satisfy the requirements for a π^0 meson in the event selection, $N_{\text{extra}}^{\pi^0} = 0$. The maximum energy of any extra photons ($E_{\text{extra},\gamma}^{\max}$) that have not been used in reconstructing the signal final states is required to be less than 0.20 GeV . The opening angle between the missing momentum and the most energetic shower, $\theta_{\vec{p}_{\text{miss}},\gamma}$, is required to satisfy $\cos \theta_{\vec{p}_{\text{miss}},\gamma} < 0.69$ (0.54) for $D^+ \rightarrow K^- \pi^+ \pi^0 \mu^+ \nu_\mu$ ($D^0 \rightarrow K^- \pi^+ \pi^- \mu^+ \nu_\mu$).

The presence of the undetectable neutrino is inferred via the kinematic quantity $U_{\text{miss}} \equiv E_{\text{miss}} - |\vec{p}_{\text{miss}}|c$, where E_{miss} and \vec{p}_{miss} are the missing energy and momentum of the semimuonic candidate, respectively, calculated by $E_{\text{miss}} \equiv E_{\text{beam}} - \sum_j E_j$ and $\vec{p}_{\text{miss}} \equiv \vec{p}_D - \sum_j \vec{p}_j$ in the e^+e^- center-of-mass frame. The index j sums over the $K^-, \pi^+, \pi^{0(-)}$ and μ^+ of the signal candidate, and E_j and \vec{p}_j are the energy and momentum of the j th particle, respectively. In order to improve the U_{miss} resolution, the D energy is constrained to the beam energy and $\vec{p}_D \equiv -\hat{p}_{\bar{D}} \sqrt{E_{\text{beam}}^2/c^2 - m_D^2 c^2}$, where $\hat{p}_{\bar{D}}$ is the unit vector in the momentum direction of the ST \bar{D} , and m_D is the nominal D mass [25].

In order to suppress backgrounds from the hadronic decays $D^{+(0)} \rightarrow K^- \pi^+ \pi^+ \pi^{0(-)}$, with misidentification of a pion as a muon, the invariant mass of the $K^- \pi^+ \pi^{0(-)} \mu^+$ combination ($M_{K^- \pi^+ \pi^{0(-)} \mu^+}$), is required to be less than 1.72 (1.65) GeV/c^2 . These selection criteria have been

optimized by analyzing the inclusive MC samples with the figure-of-merit defined by $S/\sqrt{S+B}$, where S and B denote the signal and background yields, respectively.

Figure 1 shows the distributions of $M_{K^- \pi^+ \pi^{0(-)}}$ vs. U_{miss} of the accepted candidates for $D^+ \rightarrow K^- \pi^+ \pi^0 \mu^+ \nu_\mu$ and $D^0 \rightarrow K^- \pi^+ \pi^- \mu^+ \nu_\mu$ in data. Figure 2 shows the distributions of $M_{K^- \pi^+ \pi^{0(-)}}$ of $D^{+(0)} \rightarrow K^- \pi^+ \pi^{0(-)} \mu^+ \nu_\mu$ candidates, in which significant $K_1(1270)$ signals can be seen. Selected K_1 candidates must have $M_{K^- \pi^+ \pi^{0(-)}}$ within the interval $(1.163, 1.343) \text{ GeV}/c^2$, which corresponds to about $\pm 1\Gamma$ (decay width) around the K_1 nominal mass [25].

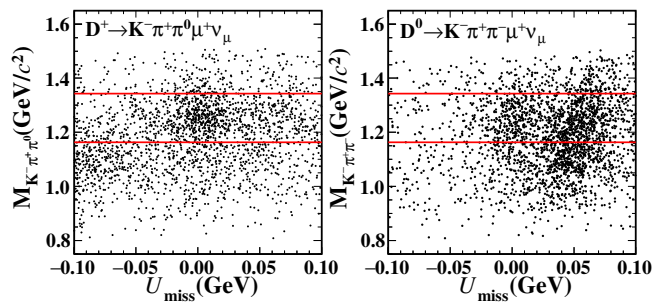


Fig. 1. The $M_{K^- \pi^+ \pi^{0(-)}}$ vs. U_{miss} distributions of the candidates for (left) $D^+ \rightarrow K^- \pi^+ \pi^0 \mu^+ \nu_\mu$ and (right) $D^0 \rightarrow K^- \pi^+ \pi^- \mu^+ \nu_\mu$. The red lines denote the accepted mass range, $(1.163, 1.343) \text{ GeV}/c^2$.

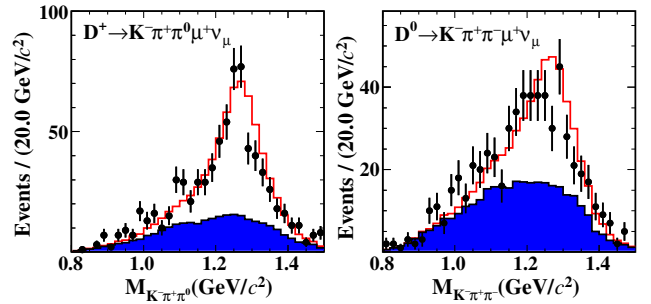


Fig. 2. The $M_{K^- \pi^+ \pi^0}$ (left) and $M_{K^- \pi^+ \pi^-}$ (right) distributions of the candidates for $D^+ \rightarrow K^- \pi^+ \pi^0 \mu^+ \nu_\mu$ and $D^0 \rightarrow K^- \pi^+ \pi^- \mu^+ \nu_\mu$. The points with error bars are data, the blue filled histograms are the simulated background, and the red line histograms are the signal MC samples. A requirement of $|U_{\text{miss}}| < 0.02 \text{ GeV}$ has been applied.

Figure 3 shows the distributions of U_{miss} of the accepted candidate events in data. Clear signals around zero are observed. The DT yields are extracted from unbinned extended maximum-likelihood fits to the U_{miss} distributions of data. In the fits, the signal shapes are described by the MC-simulated shape extracted from the signal MC events and convolved with a Gaussian function due to the resolution difference between the data and MC simulation. The combinatorial background shapes are modeled by the MC-simulated shape obtained from the inclusive MC samples. The signal yield,

the combinatorial background yield, and the Gaussian function's parameters are floated in the fits.

For $D^+ \rightarrow K^-\pi^+\pi^0\mu^+\nu_\mu$, the peaking background events from $D^+ \rightarrow K^-\pi^+\pi^+\pi^0$ (BKG II) concentrate around 0 GeV; for $D^0 \rightarrow K^-\pi^+\pi^-\mu^+\nu_\mu$, the peaking background events from $D^0 \rightarrow K^-\pi^-\eta'_{\pi^+\pi^-\gamma}$ (BKG II), $D^0 \rightarrow K^-\pi^+K^+\pi^-$ (BKG III), and $D^0 \rightarrow K^-\pi^+\pi^-\pi^+\pi^0$ (BKG IV) concentrate around 0 GeV, 0 GeV, and 0.05 GeV, respectively. All peaking background components are modeled by the MC-simulated shapes obtained from the corresponding MC samples. The backgrounds peaking near zero are convolved with the same Gaussian smearing function as the signal with their yields fixed based on MC simulations. The peaking around 0.05 GeV is convolved with a separate Gaussian function and its yield and parameters of Gaussian function are free.

In the fits, the $K^-\pi^+\pi^{0(-)}$ system is assumed to be dominated by the axial-vector meson K_1 , while other components are ignored due to limited statistics (see Fig. 1, and 2 of supplemental materials [31]). From the fits, we obtain the DT yields to be 382.8 ± 31.9 and 180.3 ± 25.9 for $D^+ \rightarrow K^-\pi^+\pi^0\mu^+\nu_\mu$ and $D^0 \rightarrow K^-\pi^+\pi^-\mu^+\nu_\mu$, respectively, where the uncertainties are statistical. Their statistical significances are estimated to be 14.0σ and 6.8σ , respectively, by comparing the likelihoods with and without the signal components included, taking into account the change in the number of degrees of freedom. After further considering the non- K_1 component of $K^-\pi^+\pi^{0(-)}$, as discussed in the systematic uncertainty part, the significances of $D^+ \rightarrow K^-\pi^+\pi^0\mu^+\nu_\mu$ and $D^0 \rightarrow K^-\pi^+\pi^-\mu^+\nu_\mu$ are 12.5σ and 6.0σ , respectively.

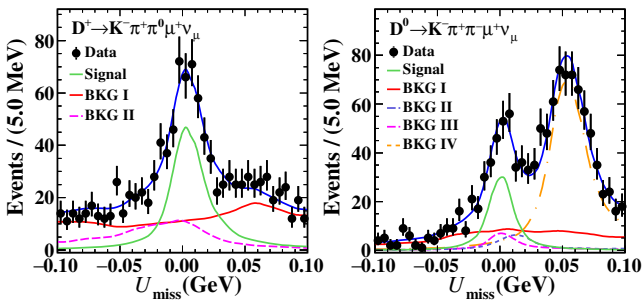


Fig. 3. Fits to the U_{miss} distributions of the candidates for (left) $D^+ \rightarrow K^-\pi^+\pi^0\mu^+\nu_\mu$ and (right) $D^0 \rightarrow K^-\pi^+\pi^-\mu^+\nu_\mu$. The points with error bars are data. The blue solid curves are the total fits, the green solid curves denote the semimuonic signal shapes, and the red solid curves are from the combinatorial background shapes (BKG I). In the left plot, the magenta dashed curve is the background contribution from $D^+ \rightarrow K^-\pi^+\pi^+\pi^0$ (BKG II). In the right plot, the violet and magenta dashed curves are the background contributions from $D^0 \rightarrow K^-\pi^-\eta'_{\pi^+\pi^-\gamma}$ (BKG II) and $D^0 \rightarrow K^-\pi^+K^+\pi^-$ (BKG III), respectively. The orange dashed curves is the background contribution from $D^0 \rightarrow K^-\pi^+\pi^-\pi^+\pi^0$ (BKG IV).

The DT efficiencies, $\varepsilon_{\text{DT}}^i$, obtained from signal MC samples with the same analysis procedures as for data, are summarized in Table 1 of Ref. [31]. The averaged signal efficiencies in the presence of the ST \bar{D} mesons are $(8.45 \pm 0.05)\%$ and $(10.92 \pm 0.07)\%$ for $D^+ \rightarrow K^-\pi^+\pi^0\mu^+\nu_\mu$ and $D^0 \rightarrow K^-\pi^+\pi^-\mu^+\nu_\mu$, respectively. These efficiencies include correction factors which are discussed later. The final signal efficiency, ε_{sig} , includes the BF of $\pi^0 \rightarrow \gamma\gamma$ [25]. The reliability of the MC simulation has been verified by the agreement of the distributions of the momenta and $\cos\theta$ of K^- , π^+ , $\pi^{0(-)}$, and μ^+ with the data.

By inserting N_{DT} , ε_{sig} , and $N_{\text{ST}}^{\text{tot}}$ into Eq. (1), we determine the product of \mathcal{B}_{SL} and \mathcal{B}_{K_1} [25] to be

$$\mathcal{B}_{\text{SL}}^+ \mathcal{B}_{K_1}^0 = (10.92 \pm 0.91^{+0.82}_{-1.26}) \times 10^{-4},$$

$$\mathcal{B}_{\text{SL}}^0 \mathcal{B}_{K_1}^- = (2.62 \pm 0.38^{+0.17}_{-0.29}) \times 10^{-4},$$

where the first and second uncertainties are statistical and systematic, respectively. All related numbers are summarized in Table 1.

The systematic uncertainties in the BF measurement, which are assigned relative to the measured BFs, are discussed below. The DT method ensures that most uncertainties arising from the ST selection cancel. The uncertainty associated with the ST yield $N_{\text{ST}}^{\text{tot}}$, is assigned as 0.3% after varying the signal and background shapes in the M_{BC} fit.

The uncertainties associated with the efficiencies of μ^+ tracking, K^- tracking and PID, π^+ tracking and PID, and π^0 reconstruction are investigated using data and MC samples of $e^+e^- \rightarrow \gamma\mu^+\mu^-$ events and DT $D\bar{D}$ hadronic events ($\bar{D}^0 \rightarrow K^+\pi^-$, $\bar{D}^0 \rightarrow K^+\pi^-\pi^0$, and $\bar{D}^0 \rightarrow K^+\pi^+\pi^-\pi^-$ vs. $D^0 \rightarrow K^-\pi^+$, $D^0 \rightarrow K^-\pi^+\pi^+\pi^-$, and $D^0 \rightarrow K^-\pi^+\pi^0$, and $D^- \rightarrow K^+\pi^-\pi^-$ vs. $D^+ \rightarrow K^-\pi^+\pi^+$). We assign the uncertainties associated with the μ^+ tracking, K^- tracking (PID), π^+ tracking (PID) and π^0 reconstruction to be 1.0%, 0.5% (0.5%), 0.5% (0.5%) and 2.0%, respectively.

In the studies of μ^+ PID efficiencies, the 2D (momentum and $\cos\theta$) PID efficiencies of data and MC simulation of $e^+e^- \rightarrow \gamma\mu^+\mu^-$ events are reweighted to match those of $D^{(0)} \rightarrow \bar{K}_1^0\mu^+\nu_\mu$ decays. The efficiency differences are $-(1.5 \pm 0.4)\%$ and $-(2.3 \pm 0.4)\%$ for $D^+ \rightarrow \bar{K}_1^0\mu^+\nu_\mu$ and $D^0 \rightarrow \bar{K}_1^-\mu^+\nu_\mu$, respectively. The MC efficiencies are then corrected by these differences and used to determine the BFs of the semimuonic decays. After corrections, we assign the uncertainties associated with the μ^+ PID to be 0.4% and 0.4%, respectively. The systematic uncertainties due to the combined requirements on $E_{\text{extra}\gamma}^{\text{max}}$, $N_{\text{extra}}^{\pi^0}$, $N_{\text{extra}}^{\text{char}}$ and, separately, that on $\cos\theta_{\vec{p}_{\text{miss}},\gamma}$ are investigated using the control sample of $D^{(0)} \rightarrow K_S^0\pi^{0(-)}\mu^+\nu_\mu$. The corresponding systematic uncertainties are assigned as 3.9% and 4.0% for $D^+ \rightarrow \bar{K}_1^0\mu^+\nu_\mu$ respectively; while

Table 1. The DT yields, N_{DT} , in data, their statistical significances, the signal efficiencies, $\bar{\epsilon}_{\text{SL}}$, and the obtained BFs, \mathcal{B}_{SL} , for the two signal modes. The first and second uncertainties are statistical and systematic, respectively. The third uncertainty is from knowledge of the external BF, \mathcal{B}_{K_1} .

Signal decay	N_{DT}	Significance (σ)	$\bar{\epsilon}_{\text{SL}} (\%)$	$\mathcal{B}_{K_1} \mathcal{B}_{\text{SL}} (\times 10^{-4})$	$\mathcal{B}_{K_1} (\%)$	$\mathcal{B}_{\text{SL}} (\times 10^{-3})$
$D^+ \rightarrow \bar{K}_1^0 \mu^+ \nu_\mu$	382.8 ± 31.9	12.5	8.45 ± 0.05	$10.92 \pm 0.91^{+0.82}_{-1.26}$	46.24 ± 9.33	$2.36 \pm 0.20^{+0.18}_{-0.27} \pm 0.48$
$D^0 \rightarrow K_1^- \mu^+ \nu_\mu$	180.3 ± 25.9	6.0	10.92 ± 0.07	$2.62 \pm 0.38^{+0.17}_{-0.29}$	33.74 ± 6.54	$0.78 \pm 0.11^{+0.05}_{-0.09} \pm 0.15$

those for $D^0 \rightarrow K_1^- \mu^+ \nu_\mu$ are 2.6% and 2.3%, respectively.

To estimate the uncertainties due to the $M_{K_1^- \pi^+ \pi^0(-)} \mu^+$ requirements, we use DT samples with the signal modes replaced by $D^+ \rightarrow K_S^0 \pi^0 \mu^+ \nu_\mu$ and $D^0 \rightarrow K_S^0 \pi^- \mu^+ \nu_\mu$ and assign uncertainties of 4.2% and 2.3%, for the D^+ and D^0 modes, respectively.

To estimate the uncertainties due to the $M_{K_1^- \pi^+ \pi^0(-)}$ requirements, we remeasure the BFs with the nominal K_1 mass window half width of 0.90 GeV/ c^2 widened to 1.10 GeV/ c^2 . The differences between the average BFs and the baseline values are assigned as the systematic uncertainties, which yields 0.6% for both decay modes.

The uncertainties associated with the fits to the U_{miss} distributions are estimated to be $+0.5\%$ ($+4.4\%$) which are dominated by the uncertainty from the background shape. These systematic uncertainties are studied by altering the default MC background shape in three ways. First, alternative MC samples are used to determine the background shape, where the relative fraction of the $q\bar{q}$ background is varied within the uncertainties [32]. Second, the BFs of the major $D\bar{D}$ background sources are varied by their uncertainties [25]. Third, the non- $K_1^- (\bar{K}_1^0)$ sources of $K^- \pi^+ \pi^- (K^- \pi^+ \pi^0)$ ($+0.0\% (+0.0\%)$ ($-8.8\% (-9.0\%)$)) are the dominant uncertainties. They are assigned to be the changes of the fitted DT yields after fixing nonresonant components by referring to the nonresonant fraction in $B \rightarrow J/\psi \bar{K}\pi\pi$ [33], since the nonresonant fraction in $D^{0(+)} \rightarrow \bar{K}\pi e^+ \nu_e$ [34, 35] is close to that in $B^+ \rightarrow J/\psi \bar{K}\pi$ [36].

The uncertainties related to the signal MC model are estimated to be 1.0% (1.0%), which correspond to the differences of the baseline signal efficiencies and those obtained with the signal MC samples after varying the input generator parameters by $\pm 1\sigma$. The uncertainty due to the limited MC statistics is 0.4% (0.4%).

The total systematic uncertainties are $+7.5\%$ and $+6.5\%$ for $D^+ \rightarrow \bar{K}_1^0 \mu^+ \nu_\mu$ and $D^0 \rightarrow K_1^- \mu^+ \nu_\mu$, respectively, obtained by adding all the individual contributions in quadrature. All systematic uncertainties are summarized in Table 2.

Using the world average of $\mathcal{B}_{K_1 \rightarrow K_1^- \pi^+ \pi^0} = (46.24 \pm 9.33)\%$ [37] $\mathcal{B}_{K_1 \rightarrow K_1^- \pi^+ \pi^-} = (33.74 \pm 6.54)\%$ [38], we obtain:

$$\mathcal{B}_{D^+ \rightarrow \bar{K}_1^0 \mu^+ \nu_\mu} = (2.36 \pm 0.20^{+0.18}_{-0.27} \pm 0.48) \times 10^{-3},$$

$$\mathcal{B}_{D^0 \rightarrow K_1^- \mu^+ \nu_\mu} = (0.78 \pm 0.11^{+0.05}_{-0.09} \pm 0.15) \times 10^{-3},$$

Table 2. Systematic uncertainties in % for the BF measurements.

Source	$\bar{K}_1^0 \mu^+ \nu_\mu$	$K_1^- \mu^+ \nu_\mu$
$N_{\text{ST}}^{\text{tot}}$	0.3	0.3
μ^+ tracking	1.0	1.0
K^-, π^\pm tracking	1.0	1.5
K^-, π^\pm PID	1.0	1.5
π^0 reconstruction	2.0	...
μ^+ PID	0.4	0.4
$E_{\text{extra}\gamma}^{\text{max}}, N_{\pi^0}^{\text{extra}}, N_{\text{char}}^{\text{extra}}$	3.9	2.6
$\cos \theta_{\vec{p}_{\text{miss}}, \gamma}$	4.0	2.3
$M_{K_1^- \pi^+ \pi^0(-)} \mu^+$ requirement	4.2	2.3
$M_{K_1^- \pi^+ \pi^0(-)}$ requirement	0.6	0.6
U_{miss} fit	$^{+0.5}_{-8.8}$	$^{+4.4}_{-10.0}$
Signal model	1.0	1.0
MC statistics	0.4	0.4
Total	$^{+7.5}_{-11.6}$	$^{+6.5}_{-11.1}$

where the third uncertainty is from the input BFs.

To summarize, by analyzing 7.93 fb^{-1} of $e^+ e^-$ collisions data taken at $\sqrt{s} = 3.773 \text{ GeV}$, we report the first observation of $D^+ \rightarrow \bar{K}_1^0 \mu^+ \nu_\mu$ and $D^0 \rightarrow K_1^- \mu^+ \nu_\mu$ with statistical significances of 12.5σ and 6.0σ , respectively. Their decay BFs are determined to be $\mathcal{B}[D^+ \rightarrow \bar{K}_1^0 \mu^+ \nu_\mu] = (2.36 \pm 0.20^{+0.18}_{-0.27} \pm 0.48) \times 10^{-3}$ and $\mathcal{B}[D^0 \rightarrow K_1^- \mu^+ \nu_\mu] = (0.78 \pm 0.11^{+0.05}_{-0.09} \pm 0.15) \times 10^{-3}$. Table 3 shows the comparison of the measured BFs with several theoretical calculations. Because the BFs predicted in theory are sensitive to the K_1 mixing angle, our BFs provides some information on the K_1 mixing angle. Our BFs disfavor the theoretical calculations from LCSR [11] and CLFQM [12], which are under the assumption of the mixing angle $\theta_{K_1} = -(34 \pm 13)^\circ$, by more than 5σ .

Combining the BFs measured in this work and the BFs of $\mathcal{B}[D^+ \rightarrow \bar{K}_1^0 e^+ \nu_e] = (2.30 \pm 0.26^{+0.18}_{-0.21} \pm 0.25) \times 10^{-3}$ [39] and $\mathcal{B}[D^0 \rightarrow K_1^- e^+ \nu_e] = (1.09 \pm 0.13^{+0.09}_{-0.13} \pm 0.12) \times 10^{-3}$ [40] reported in the previous BESIII analysis, we determine the BF ratios ($\mathcal{R}_{\mu/e}^D = \frac{\mathcal{B}[D \rightarrow \bar{K}_1^0 \mu^+ \nu_\mu]}{\mathcal{B}[D \rightarrow K_1^- e^+ \nu_e]}$) to be $\mathcal{R}_{\mu/e}^{D^+} = 1.03 \pm 0.14^{+0.11}_{-0.15}$ and $\mathcal{R}_{\mu/e}^{D^0} = 0.74 \pm 0.13^{+0.08}_{-0.13}$. Here, the systematic uncertainties in ST yields, K^-/π^\pm tracking and PID, and π^0 reconstruction cancel. These are consistent with theoretical predictions

Table 3. Comparison of the BFs measured in this work with the predicted values for $D^{+(0)} \rightarrow \bar{K}_1 \mu^+ \nu_\mu (\times 10^{-3})$ from various theories with differences given in units of standard deviations.

Decay	θ_{K_1}	CLFQM [10]	3PSR [9]	LCSR [11]	LCSR [11]	LCSR [11]	CLFQM [12]	LFQM [12]	LCSR [12]	This work
		33°	37°		-(34 ± 13)°		45°			-
$D^+ \rightarrow \bar{K}_1^0 \mu^+ \nu_\mu$	Predicted	2.60 ± 0.30	2.70 ± 0.25	18.59 ± 0.31	16.86 ± 0.27	19.73 ± 0.32	$5.9_{-0.11}^{+0.47}$	$3.7_{-0.41}^{+0.00}$	$1.4_{-0.27}^{+0.15}$	$2.36 \pm 0.20_{-0.27}^{+0.18} \pm 0.48$
	Deviation (σ)	0.4	0.6	27.3	25.2	29.0	6.8	2.6	1.8	
$D^0 \rightarrow K_1^- \mu^+ \nu_\mu$	Predicted	-	1.03 ± 0.1	8.09 ± 0.15	6.78 ± 0.12	8.92 ± 0.16	$2.3_{-0.44}^{+0.19}$	$1.5_{-0.16}^{+0.00}$	$0.54_{-0.11}^{+0.06}$	$0.78 \pm 0.11_{-0.09}^{+0.05} \pm 0.15$
	Deviation (σ)	-	1.1	28.6	25.1	31.1	5.4	2.8	1.1	

based on μ -e LFU in $D^{+(0)} \rightarrow \bar{K}_1 \ell^+ \nu_\ell$ decays within current uncertainties. Using the BFs of $D^0 \rightarrow K_1^- \mu^+ \nu_\mu$ and $D^+ \rightarrow \bar{K}_1^0 \mu^+ \nu_\mu$ measured in this work as well as the world-average lifetimes of the D^0 and D^+ mesons [25], we determine the partial decay width ratio $\Gamma[D^+ \rightarrow \bar{K}_1^0 \mu^+ \nu_\mu]/\Gamma[D^0 \rightarrow K_1^- \mu^+ \nu_\mu] = 1.22 \pm 0.10_{-0.09}^{+0.06}$, which is consistent with unity as predicted by isospin conservation.

I. ACKNOWLEDGEMENTS

The BESIII Collaboration thanks the staff of BEPCII and the IHEP computing center for their strong support. This work is supported in part by National Key R&D Program of China under Contracts Nos. 2023YFA1606000; National Natural Science Foundation of China (NSFC) under Contracts Nos. 11635010, 11735014, 11935015, 11935016, 11935018, 12025502, 12035009, 12035013, 12061131003, 12192260, 12192261, 12192262, 12192263, 12192264, 12192265, 12221005,

12225509, 12235017, 12361141819; the Chinese Academy of Sciences (CAS) Large-Scale Scientific Facility Program; the CAS Center for Excellence in Particle Physics (CCEPP); Joint Large-Scale Scientific Facility Funds of the NSFC and CAS under Contract No. U1832207; 100 Talents Program of CAS; The Institute of Nuclear and Particle Physics (INPAC) and Shanghai Key Laboratory for Particle Physics and Cosmology; German Research Foundation DFG under Contracts Nos. 455635585, FOR5327, GRK 2149; Istituto Nazionale di Fisica Nucleare, Italy; Ministry of Development of Turkey under Contract No. DPT2006K-120470; National Research Foundation of Korea under Contract No. NRF-2022R1A2C1092335; National Science and Technology fund of Mongolia; National Science Research and Innovation Fund (NSRF) via the Program Management Unit for Human Resources & Institutional Development, Research and Innovation of Thailand under Contract No. B16F640076; Polish National Science Centre under Contract No. 2019/35/O/ST2/02907; The Swedish Research Council; U. S. Department of Energy under Contract No. DE-FG02-05ER41374.

-
- [1] M. Suzuki, *Phys. Rev. D* **47**, 1252 (1993).
[2] H. Hatanaka and K. C. Yang, *Phys. Rev. D* **77**, 094023 (2008); [erratum: *Phys. Rev. D* **78**, 059902 (2008).]
[3] H. Y. Cheng and C. K. Chua, *Phys. Rev. D* **69**, 094007 (2004); [erratum: *Phys. Rev. D* **81**, 059901 (2010).]
[4] H. Y. Cheng and C. W. Chiang, *Phys. Rev. D* **81**, 074031 (2010).
[5] G. Y. Wang, L. Roca, E. Wang, W. H. Liang and E. Oset, *Eur. Phys. J. C* **80**, 388 (2020).
[6] H. Y. Cheng, *Phys. Rev. D* **67**, 094007 (2003).
[7] N. Isgur, D. Scora, B. Grinstein and M. B. Wise, *Phys. Rev. D* **39**, 799 (1989).
[8] D. Scora and N. Isgur, *Phys. Rev. D* **52**, 2783 (1995).
[9] R. Khosravi, K. Azizi and N. Ghahramany, *Phys. Rev. D* **79**, 036004 (2009).
[10] H. Y. Cheng and X. W. Kang, *Eur. Phys. J. C* **77**, 587 (2017); [erratum: *Eur. Phys. J. C* **77**, 863 (2017).]
[11] S. Momeni and R. Khosravi, *J. Phys. G* **46**, 105006 (2019).
[12] L. Bian, L. Sun and W. Wang, *Phys. Rev. D* **104**, 053003 (2021).
[13] Y. S. Amhis *et al.* (HFLAV Collaboration), *Phys. Rev. D* **107**, 052008 (2023).
[14] A. M. Coutinho, A. Crivellin and C. A. Manzari, *Phys. Rev. Lett.* **125**, 071802 (2020).
[15] A. Crivellin and M. Hoferichter, *Phys. Rev. Lett.* **125**, 111801 (2020).
[16] S. Fajfer, I. Nisandzic and U. Rojec, *Phys. Rev. D* **91**, 094009 (2015).
[17] B. C. Ke, J. Koponen, H. B. Li and Y. H. Zheng, *Ann. Rev. Nucl. Part. Sci.* **73**, 285 (2023).
[18] M. Ablikim *et al.* (BESIII Collaboration), *Chin. Phys. C* **37**, 123001 (2013); *Phys. Lett. B* **753**, 629-638 (2016), [erratum: *Phys. Lett. B* **812**, 135982 (2021)]; *Chin. Phys. C* **48**, 123001 (2024).
[19] M. Ablikim *et al.* (BESIII Collaboration), *Nucl. Instrum. Meth. A* **614**, 345 (2010).
[20] X. Li *et al.* *Radiat. Detect. Technol. Methods* **1**, 13 (2017); Y. X. Guo *et al.* *Radiat. Detect. Technol. Methods* **1**, 15 (2017); P. Cao *et al.* *Nucl. Instrum. Meth. A* **953**, 163053 (2020).
[21] S. Agostinelli *et al.* (GEANT4 Collaboration), *Nucl. Instrum. Meth. A* **506**, 250 (2003).
[22] S. Jadach, B. F. L. Ward and Z. Was, *Phys. Rev. D* **63**, 113009 (2001);

- Comput. Phys. Commun.* **130**, 260 (2000).
- [23] R. G. Ping, *Chin. Phys. C* **38**, 083001 (2014).
- [24] D. J. Lange, *Nucl. Instrum. Meth. A* **462**, 152 (2001); R. G. Ping, *Chin. Phys. C* **32**, 599 (2008).
- [25] R. L. Workman *et al.* (Particle Data Group), *Prog. Theor. Exp. Phys.* **2022**, 083C01 (2022) and 2023 update. *Phys. Rev. D* **99**, 011103 (2019).
- [26] J. C. Chen, G. S. Huang, X. R. Qi, D. H. Zhang and Y. S. Zhu, *Phys. Rev. D* **62**, 034003 (2000); R. L. Yang, R. G. Ping and H. Chen, *Chin. Phys. Lett.* **31**, 061301 (2014).
- [27] E. Richter-Was, *Phys. Lett. B* **303**, 163 (1993).
- [28] M. Ablikim *et al.* (BESIII Collaboration), arXiv:2503.02196 .
- [29] M. Ablikim *et al.* (BESIII Collaboration), *Phys. Rev. D* **109**, 072003 (2024).
- [30] H. Albrecht *et al.* (ARGUS Collaboration), *Phys. Lett. B* **241**, 278 (1990).
- [31] See Supplemental Material at [URL will be inserted by publisher] for further details on the ST and DT selection.
- [32] M. Ablikim *et al.* (BES Collaboration), *Phys. Lett. B* **641**, 145 (2006).
- [33] H. Guler *et al.* (Belle Collaboration), *Phys. Rev. D* **83**, 032005 (2011).
- [34] M. Ablikim *et al.* (BESIII Collaboration), *Phys. Rev. D* **99**, 011103 (2019).
- [35] M. Ablikim *et al.* (BESIII Collaboration), *Phys. Rev. D* **94**, 032001 (2016).
- [36] K. Abe *et al.* (Belle Collaboration), *Phys. Lett. B* **538**, 11 (2002).
- [37] $\mathcal{B}_{K_1 \rightarrow K^- \pi^+ \pi^0} = \frac{2}{3} \times \mathcal{B}_{K_1 \rightarrow K\rho} + \frac{4}{9} \times \mathcal{B}_{K_1 \rightarrow K^*(892)\pi} + \frac{4}{9} \times 0.93 \times \mathcal{B}_{K_1 \rightarrow K_0^*(1430)\pi}$, where K_1 denotes $\bar{K}_1(1270)^0$.
- [38] $\mathcal{B}_{K_1 \rightarrow K^- \pi^+ \pi^-} = \frac{1}{3} \times \mathcal{B}_{K_1 \rightarrow K\rho} + \frac{4}{9} \times \mathcal{B}_{K_1 \rightarrow K^*(892)\pi} + \frac{4}{9} \times 0.93 \times \mathcal{B}_{K_1 \rightarrow K_0^*(1430)\pi} + \mathcal{B}_{K_1 \rightarrow K^+\omega} \times \mathcal{B}_{\omega \rightarrow \pi^+ \pi^-}$ where K_1 denotes $K_1(1270)^-$.
- [39] M. Ablikim *et al.* (BESIII Collaboration), *Phys. Rev. Lett.* **123**, 231801 (2019).
- [40] M. Ablikim *et al.* (BESIII Collaboration), *Phys. Rev. Lett.* **127**, 131801 (2021).

SUPPLEMENTAL MATERIALS

Table 4 summarizes some analysis details for the single-tag D^- candidates, namely the ΔE requirements, the ST yields in data, the ST efficiencies, and the double-tag efficiencies.

Table 4. The ΔE requirements, the obtained ST $\bar{D}^0(D^-)$ yields (N_{ST}^i) in data, the ST efficiencies ($\varepsilon_{\text{ST}}^i$), and the DT efficiencies ($\varepsilon_{\text{DT}}^i$). The efficiencies do not include the branching fractions of the K_S^0 and π^0 decays. The uncertainties are statistical only.

Tag mode	ΔE (GeV)	$N_{\text{ST}}^i (\times 10^3)$	$\varepsilon_{\text{ST}}^i$ (%)	$\varepsilon_{\text{DT}}^i$ (%)
$D^- \rightarrow K^+ \pi^- \pi^-$	(-0.025, 0.024)	2164.1 ± 1.6	51.17 ± 0.01	8.87 ± 0.09
$D^- \rightarrow K_S^0 \pi^-$	(-0.025, 0.026)	250.4 ± 0.5	50.74 ± 0.02	9.17 ± 0.09
$D^- \rightarrow K^+ \pi^- \pi^- \pi^0$	(-0.057, 0.046)	689.0 ± 1.2	25.50 ± 0.01	7.74 ± 0.12
$D^- \rightarrow K_S^0 \pi^- \pi^0$	(-0.062, 0.049)	558.5 ± 0.9	26.28 ± 0.01	8.47 ± 0.12
$D^- \rightarrow K_S^0 \pi^- \pi^- \pi^+$	(-0.028, 0.027)	300.5 ± 0.7	29.01 ± 0.01	8.13 ± 0.12
$D^- \rightarrow K^+ K^- \pi^-$	(-0.024, 0.023)	187.4 ± 0.5	41.06 ± 0.02	7.83 ± 0.10
$\bar{D}^0 \rightarrow K^+ \pi^-$	(-0.027, 0.027)	1449.3 ± 1.3	65.34 ± 0.01	11.72 ± 0.09
$\bar{D}^0 \rightarrow K^+ \pi^- \pi^0$	(-0.062, 0.049)	2913.2 ± 2.0	35.59 ± 0.01	11.16 ± 0.12
$\bar{D}^0 \rightarrow K^+ \pi^+ \pi^- \pi^-$	(-0.026, 0.024)	1944.2 ± 1.6	40.83 ± 0.01	9.95 ± 0.11

Figure 4 and 5 shows the distributions of $M_{K-\pi^+}$, $M_{K-\pi^0(-)}$ and $M_{\pi^+\pi^0(-)}$ for $D^+ \rightarrow K^-\pi^+\pi^0\mu^+\nu_\mu$ and $D^0 \rightarrow K^-\pi^+\pi^-\mu^+\nu_\mu$ candidates, respectively. Results from the data and the inclusive MC sample are overlaid.

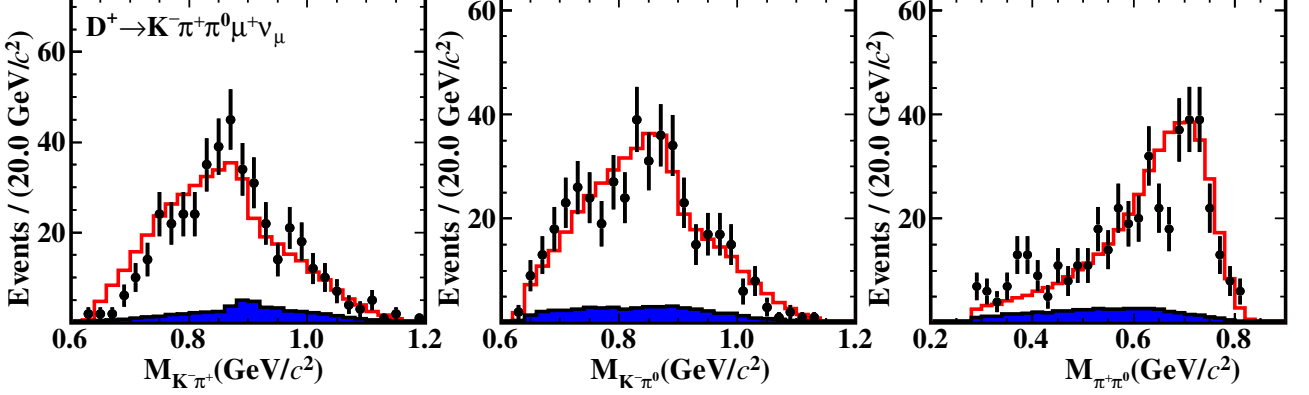


Fig. 4. Comparison of $M_{K^-\pi^+}$ (left), $M_{K^-\pi^0}$ (center) and $M_{\pi^+\pi^0}$ (right) of the candidates for $D^+ \rightarrow K^-\pi^+\pi^0\mu^+\nu_\mu$. The points with error bars are data, the blue filled histograms are the simulated background, and the red line histograms are the signal MC samples. A requirement of $|U_{\text{miss}}| < 0.02 \text{ GeV}$ has been applied.

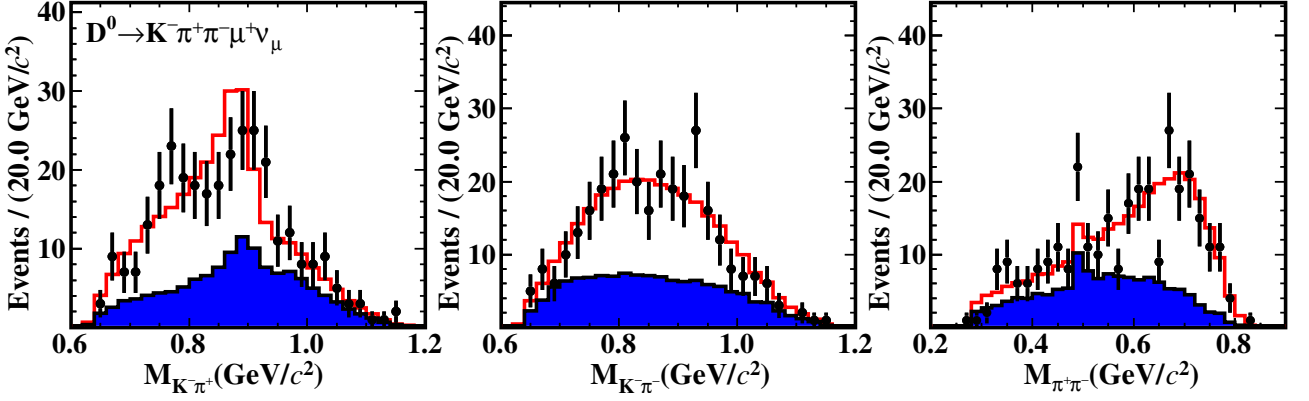


Fig. 5. Comparison of $M_{K^-\pi^+}$ (left), $M_{K^-\pi^-}$ (center) and $M_{\pi^+\pi^-}$ (right) of the candidates for $D^0 \rightarrow K^-\pi^+\pi^-\mu^+\nu_\mu$. The points with error bars are data, the blue filled histograms are the simulated background, and the red line histograms are the signal MC samples. A requirement of $|U_{\text{miss}}| < 0.02 \text{ GeV}$ has been applied.